

# *In situ* measurements of HCl during plasma etching of poly-silicon using a diode laser absorption sensor

Suhong Kim<sup>1</sup>, Pete Klimecky<sup>2</sup>, Jay B Jeffries<sup>1</sup>, Fred L Terry Jr<sup>2</sup>  
and Ronald K Hanson<sup>1</sup>

<sup>1</sup> Stanford University, High Temperature Gasdynamics Laboratory, Mechanical Engineering Department, Building 520, Stanford, CA 94305-3032, USA

<sup>2</sup> University of Michigan, Center for Integrated Micro Systems, EECS Department, 2408 EECS Building, 1301 Beal Avenue, Ann Arbor, MI 48109-2122, USA

E-mail: suhong@stanford.edu

Received 15 May 2003, in final form 2 July 2003, accepted for publication 4 July 2003

Published 29 July 2003

Online at [stacks.iop.org/MST/14/1662](http://stacks.iop.org/MST/14/1662)

## Abstract

Tunable diode laser absorption spectroscopy is used to monitor hydrogen chloride (HCl) concentration in a commercial, high-density, low-pressure plasma reactor during plasma etching. A near-infrared diode laser is used to scan the P(4) transition in the first overtone of HCl near 1.79  $\mu\text{m}$  to measure changes in HCl levels. A variety of HBr and  $\text{Cl}_2$  feedstock recipes are investigated at a process pressure of 10 mTorr as a function of rf power transformer coupled plasma, bias power and the total flow rate. Using 50 ms averaging and a signal modulation technique, we estimate a minimum detectivity of  $4 \times 10^{-6}$  in peak absorbance, which corresponds to an HCl number density of  $\sim 2 \times 10^{11} \text{ cm}^{-3}$ . The diode-laser based HCl sensor is sufficiently sensitive to detect small concentration variations and HCl concentration correlates with poly-Si etch rate for the conditions studied. These measurements demonstrate the feasibility of a real-time diode laser-based sensor for etch rate monitoring and the potential for process control.

**Keywords:** tunable diode lasers, hydrogen chloride sensor, plasma etching, etch rate monitor

## 1. Introduction

Tunable diode laser absorption spectroscopy (TDLAS) is a well established technique for detection of trace gas [1]. The technique is especially well suited to measurements in chemically reactive environments because no physical probe is required in the test gases. Modulation methods [2, 3] significantly increase the sensitivity compared to direct absorption at the cost of signal calibration. For the poly-silicon (poly-Si) etch application presented here, we use wavelength-modulated absorption of diode laser light to monitor hydrogen chloride (HCl) in a commercial plasma reactor (Lam Research 9400SE) of the type typically used for manufacturing integrated circuits (IC).

Chlorine-based etch recipes are generally preferred over fluorine-based recipes for modern poly-Si etching due to higher selectivity, and good anisotropic profiles while maintaining acceptable etch rates. For many recipes, HBr is added to the  $\text{Cl}_2$  main etch step to help suppress isotropic undercut by passivating films on the trench sidewalls [4]. HBr also helps maintain clean bases at the bottom of etch trenches and minimizes micro-trench features. Therefore, combinations of  $\text{Cl}_2$ /HBr flow ratios are explored for this study as the main etch feedstock gas.

In the  $\text{Cl}_2$ /HBr plasma, the HCl acts as a reservoir reducing the concentration of atomic chlorine species, such as Cl and  $\text{Cl}^+$ , in the plasma; these atomic reactants are largely

responsible for the reactive etching to form the  $\text{SiCl}_4$  etch product. Therefore the HCl is a measure of the chlorine that is unavailable to etch silicon, and we expect the HCl concentration to anticorrelate with active atomic Cl species. Previous work in a similar etch reactor has established that the HCl partial pressure is negatively related to the average etch rate in the low  $\text{Cl}_2$  flow rate range [5]. In this paper, we report the measurements of HCl number density by wavelength modulation spectroscopy (wms) scanning P(4) in the first overtone band near  $1.79 \mu\text{m}$ . We present three examples of this sensor during poly-Si etching in  $\text{Cl}_2/\text{HBr}$  plasmas: (1) calibration of the  $2f$  wavelength modulation signal with direct absorption measurements; (2) variation of the HCl concentration with process parameters in a Lam Research 9400SE reactor including transformer-coupled plasma (TCP), total flow rate and bias effects and (3) correlation of time-varying chemical concentrations with etch rate and plasma density variations.

The sensor found a significant HCl concentration transient during the first etch step following a typical fluorine-based plasma clean cycle. Other sensors on the same reactor confirmed a time-varying etch rate correlating with the HCl concentration variation, suggesting that the HCl sensor could be used to control poly-Si etch rate transients.

## 2. Background

Plasma etching is a critical step in the IC manufacturing process to precisely imprint photolithographic device patterns into the thin film layers on a semiconductor wafer. Accurate pattern transfer is achieved with acceptable wafer throughput when the process has a high etch rate, good material selectivity between layers, and highly anisotropic etch profiles [6, 7]. Plasma etching of the poly-Si system with reactive halogen species generally suits these stated criteria. This makes poly-Si widely used as a gate material in metal-oxide-semiconductor field effect transistor (MOSFET) devices for computer chip memory such as DRAM, as well as in microelectromechanical systems (MEMS) [8].

To initiate and maintain the plasma discharge, external energy is supplied by a radio frequency (rf) generator capable of producing high-density plasmas at low pressures. For the work presented here, a Lam 9400SE TCP reactor is used for the poly-Si etching. The rf power, termed the TCP, dissociates the feedstock gas molecules and some of these reactive atoms are ionized. Neutral halogen atoms attack the poly-Si substrate and provide an isotropic etch component to the process. The positively charged halogen ions are accelerated through a large potential to the wafer where they impact the surface with high energy and reactively etch the surface. For the configuration of the Lam 9400SE reactor, a second power supply (bias power) is included on the lower electrode to better control the ion bombardment energy. The high-energy ion bombardment adds a vertical etch component to the poly-Si etch mechanism, generating a highly anisotropic etch profile.

Modern high-speed semiconductor devices with small feature sizes require highly anisotropic etching profiles and reproducibly high etch rates. Therefore, accurate control of the etch rate and profile are some of the most important objectives for the semiconductor industry [9]. Current state-of-the-art IC

devices have a critical dimension (CD) scale of 130 nm. Future generation chips are projected to reduce the CD to 9 nm by 2016 [9]. In order to accurately control the manufacture of such small features, the concentration of specific reactive species in the glow discharge as well as the ion density and bombardment energy needs to be carefully monitored. Development of accurate, reliable, cost-effective sensors for these tasks has thus far significantly impeded the implementation of direct feedback control for plasma etching processes. TDLAS offers another potential detection method for the next generation of reliable, repeatable, controlled etch processes.

Two types of sensor are currently widely used in plasma diagnostics: impedance probes and optical sensors. Probe diagnostics, such as Langmuir probes, are well established and powerful diagnostic tools. A metal probe is inserted into the chamber and in electrical contact with the plasma. From the measured current and voltage relation induced on the probe, the electron energy and the electron number density can be deduced. However, these probe techniques are intrusive to the plasma and disturb process performance and plasma uniformity. In addition, due to finite probe size, two-dimensional particle trajectory analysis is sometimes necessary for accurate measurements, making them poor diagnostics on a temporal scale.

The plasma reactor used for this study is equipped with a newly developed probe to monitor plasma density, called a broadband rf peak resonance absorption sensor [10–12]. Based on microwave resonance cavity perturbation theory, the broadband rf sensor monitors resonance peak frequencies as a function of plasma conditions, and from the relative shift in these peak absorption resonance positions determines the relative plasma density [13]. This technique is minimally intrusive to the chamber since the probe is inserted only a few centimetres into the chamber wall, and it is not in direct contact with the plasma, therefore the process parameters at the wafer are unaffected by the probe presence. This probe is used in this work to monitor and correlate the changes in electron density with the variation in HCl number density obtained by TDLAS.

Optical diagnostics are effective non-intrusive techniques which are especially well suited for chemically complex discharges. Optical emission spectroscopy (OES) is a typical method of monitoring plasmas, because emissions are strong in high-density plasmas, and they change drastically with small changes in operating conditions. However, for quantitative measurements of neutral species concentrations, an inert trace gas with similar excitation pathways, such as argon, must be incorporated in the feedstock gas supply. Measuring the ratio of the emission intensity of a gas of interest and that of a trace gas is called optical actinometry, and was pioneered for quantitative fluorine concentration [14]. Gottscho and Donnelly [15] first explored the suitability of Cl for actinometry in 1984. Bogart and Donnelly [16] and Ullal *et al* [17] applied optical actinometry to measure atomic chlorine (Cl) and molecular chlorine ( $\text{Cl}_2$ ) concentrations in a  $\text{Cl}_2$  plasma, and studies by Donnelly [18] and Malyshev and Donnelly [19] also documented chlorine actinometry measurements.

HCl is problematic to measure during plasma etching with OES due to the poor energy match of the HCl molecular transitions with an inert gas actinometer. Diode laser-based

absorption sensors have previously been used to monitor various plasma species because of the high sensitivity, simplicity and robustness of the design. Sun *et al* [20, 21] employed diode laser sensors in a plasma reactor to detect the etch endpoint in an SF<sub>6</sub> plasma environment. Chou *et al* [22] used wms with time division multiplexing to measure hydrogen bromide (HBr) and rotational temperature. We employ a similar modulation spectroscopy technique here to monitor HCl concentration and translational temperature.

### 3. Sensor design

The absorption of the diode laser light is described by the Beer-Lambert expression:

$$\frac{I_v}{I_0} = \exp(-S_i n_i \phi_v L) \quad (1)$$

where  $S_i$  is the line strength,  $n_i$  is the number density of the absorbing species,  $\phi_v$  is the lineshape function and  $L$  is the optical path length. At the low pressures of this experiment, the lineshape is dominated by Doppler broadening and a direct absorption measurement scanning the wavelength across the lineshape provides the gas temperature and HCl concentration without calibration. Unfortunately, for many of the etch conditions studied here the direct absorption has insufficient signal-to-background ratio, and wavelength modulation is used to increase the sensitivity at the cost of a separate calibration measurement. Frequency modulation spectroscopy or wms is routinely used for sensitive diode laser measurements, and the interested reader is referred to complete descriptions in the literature [2, 3]. Briefly, sinusoidal modulation is applied to the laser wavelength, and the measurement band is shifted to a narrow band around the harmonics of the modulation frequency. In this experiment we detect the second harmonic of the modulation ( $2f$ ). This avoids low-frequency noise sources, improves the determination of  $I_0$  and simplifies the rapid signal processing. In practical applications, broadband optical scattering and other losses introduce noise in the baseline fit used to determine  $I_0$ , and this limits the minimum detectable absorbance of the sensor. We monitor the P(4) transition in the first overtone of HCl, and for these experiments the product  $Sn\phi L$  is less than 0.01. For these small values of absorbance, the  $2f$  signal is directly proportional to the number density of HCl.

The quantitative spectroscopy of the vibrational transitions of HCl is well known [23–25], and line strengths are shown in figure 1(a). The fundamental band near 3.4  $\mu\text{m}$  is 50 times stronger than the first overtone; however, mid-IR laser and detector technology is not nearly as well developed as that for the near-IR region. Thus, for this work, the P(4) transition in the first overtone was selected where a room-temperature, single-mode distributed feedback (DFB) diode laser near 1.79  $\mu\text{m}$  was available.

The gas temperature in low-pressure fluorocarbon etching plasmas is only slightly higher than that of the etcher chamber, as was previously demonstrated in a similar etch reactor (and conditions) [22] and in measurements of the translational temperature in a fluorocarbon etcher [26]. Figure 1(b) shows the temperature variation of the P(4) transition of HCl overtone as calculated over the range 300–550 K from the Hitran 96

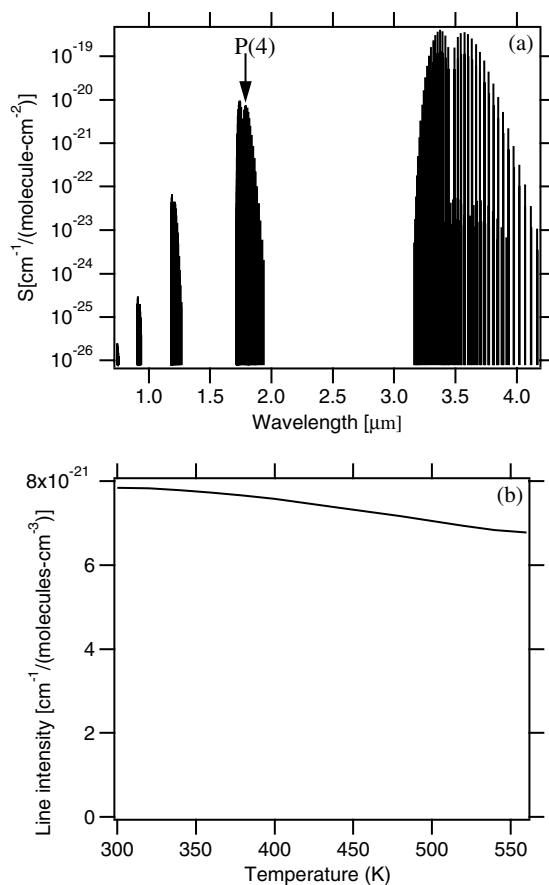


**Figure 1.** (a) Absorption line strength for HCl vibration/rotation transitions versus wavelength. (b) Line strength of the P(4) transition of the first overtone near 1.79  $\mu\text{m}$  versus temperature from the Hitran 96 database.

database [27]. In these experiments the etcher chamber is at 330 K and from the literature measurements we estimate that the gas temperature lies between 360 and 500 K. Even without correction for temperature, the HCl concentrations of the plasma can be monitored within  $\pm 5\%$  using the single laser monitoring the P(4) transition. If we correct the data using the temperature determined from direct absorption lineshapes, this uncertainty is reduced to  $\pm 2\%$ . Thus, HCl concentration can be measured in these fluorocarbon Si etch low-pressure plasmas with a single laser absorption sensor monitoring only one transition.

### 4. Experimental arrangement

The measurements were performed in a Lam Research 9400SE TCP etcher at the University of Michigan. The test wafers were 150 mm Si substrates with a blanket 5 kÅ poly-Si layer on a 300 Å SiO<sub>2</sub> layer which assists in pre- and post-etch optical measurement of poly-Si thickness. All experiments etched at 10 mTorr chamber pressure with the ratio of Cl<sub>2</sub>:HBr feedstock varied from 0:100 to 100:0 while holding the total gas flow rate constant at 100 sccm. To facilitate OES measurements, 5% Ar gas is added to the recipes. The upper electrode TCP power is set to 250 W and the lower electrode bias power is set to 180 W. The lower electrode and chamber temperature is maintained at 60 °C and the feedstock gas temperature is maintained at 45 °C;

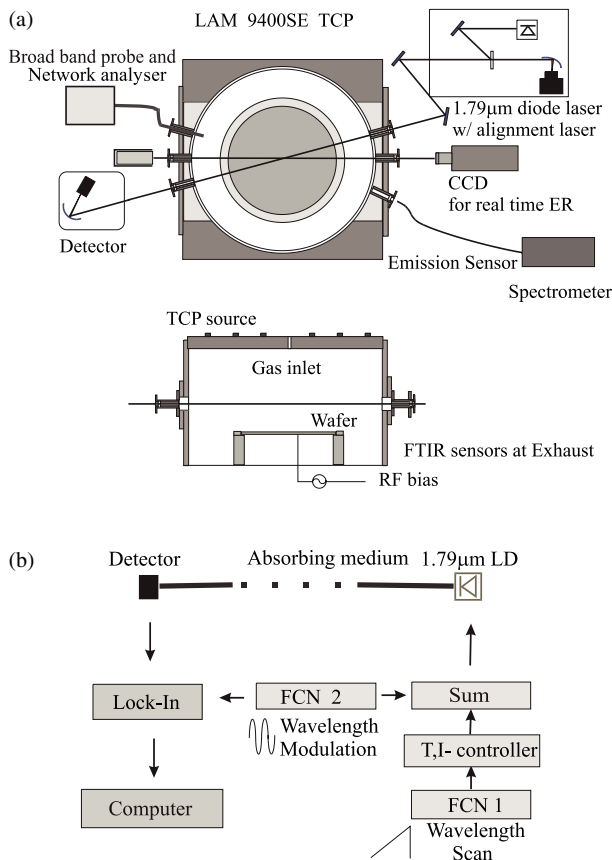


**Figure 2.** (a) Schematic experimental set-up: four real-time measurements—RTSE, broadband RF, FTIR and TDLAS. (b) Modulation scheme for TDLAS measurements.

from the TDLAS measurements described below, we find these values are 50–100 °C lower than the neutral gas temperature in the plasma.

Figure 2(a) shows a schematic of the chamber and the available array of diagnostics, and figure 2(b) depicts the TDLAS HCl sensor in detail. The near-infrared (NIR) laser beam is collimated, directed across the wafer and focused onto a detector. To reduce optical interference such as Fabry–Perot fringes, reflection optics are chosen over transmission optics. The laser output is collimated using an off-axis parabolic mirror, and a confocal mirror focuses the laser beam onto a fast detector (35 MHz, extended InGaAs). The sapphire chamber windows are wedged at 3° and installed on angled window mounts to eliminate potential Fabry–Perot etalon interference either within a window or between the two windows. A visible diode laser on the same path as the near-IR laser is used for sensor alignment. The total path length in the chamber is 48.5 cm with the beam 9.5 cm above the wafer. The focusing mirror and detector optics are placed about 2 m from the exit window to reduce the solid angle for plasma emission.

The laser wavelength is injection current tuned across the HCl transition with a 500 Hz ramp and a 10.7 MHz sinusoidal modulation is applied. The modulation index is set to 2.7, which is slightly higher than the optimal modulation index of 2.4 for a peak-to-peak measurement recommended by Silver [3]. The wms signal is detected at the second harmonic of the modulation frequency ( $2f$ ) at 21.4 MHz. This

effectively rejects the plasma emission as well as reducing the low-frequency noise.

Four other *in situ* diagnostics were available for these sensor validation experiments. A real-time spectroscopic ellipsometer (RTSE) is installed for *in situ* film thickness and etch-rate measurements. An *in situ* broadband RF probe and network analyser monitors the plasma density. An OES sensor is adopted for chlorine emission. Finally, a Fourier transform infrared (FTIR) spectroscopy sensor is installed to measure one main etch product,  $\text{SiCl}_4$ , at the turbo pump foreline exhaust. A detailed description of these diagnostics is beyond the scope of this paper and may be found in [28, 30, 31]. Comparison of experimental results from all sensors is used to provide validation of diode laser sensor interpretation.

The poly-Si etch process recipe consists of two primary steps. First the native oxide is removed with a fluorine-based plasma (typically  $\text{C}_2\text{F}_6$  or  $\text{SF}_6$  feedstock gas). This ~10–20 s etch step exposes the underlying poly-Si. The  $\text{Cl}_2/\text{HBr}$  main-etch step now begins, and the time evolution of the HCl concentration during this main-etch process is investigated in this paper. The five elements of the  $\text{Cl}_2/\text{HBr}$  main-etch step are: (1) the chamber is re-evacuated; (2) the main-etch recipe feedstock gas flows are stabilized; (3) the plasma is ignited which dissociates molecular species, (4) the bias power is applied for the main poly-Si etch (~120 s) and (5) at the completion of the main etch, the gas flows, bias power and TCP are turned off, and the chamber is evacuated again. The interaction of species on the chamber wall due to the fluorine- and chlorine-based plasmas provides a disturbance to the chamber conditions which has previously been reported [18, 28–31]. The HCl laser diode sensor also detects and tracks the effects of this chamber wall disturbance between the two plasma conditions, as will be discussed in the following section.

## 5. Experimental results

### 5.1. Measurements during the poly-Si etch cycle

Chemical reactions of the feedstock  $\text{Cl}_2/\text{HBr}$  gas mixture produce HCl in the chamber before the plasma is ignited. Presumably this chemistry is facilitated by wall reactions as the gas phase chemical reaction rates are too slow to account for this observation. We will see below that the feedstock can be quantitatively converted to HCl. First we will exploit this behaviour to test the sensor and calibrate the wavelength modulation signal.

Figure 3(a) shows the direct absorption measured in the absence of a plasma, with  $\text{Cl}_2/\text{HBr}$  gases flowing and no rf power applied. When the plasma is ignited this signal drops by a factor of 5–10 because of electron-impact dissociation of HCl and formation of  $\text{SiCl}_x\text{Br}_y$  etch products. Although during the plasma etch the smaller signal is visible, the reduced signal-to-background obscures the small changes in HCl concentration we wish to monitor. Therefore, we apply a modulation to the diode laser injection current and thus the laser wavelength. The  $2f$  wavelength-modulated lineshape is shown in figure 3(b) for the same conditions as the direct absorption in figure 3(a). When the absorbance is small the peak-to-peak amplitude of the  $2f$  wavelength modulation signal is linearly proportional

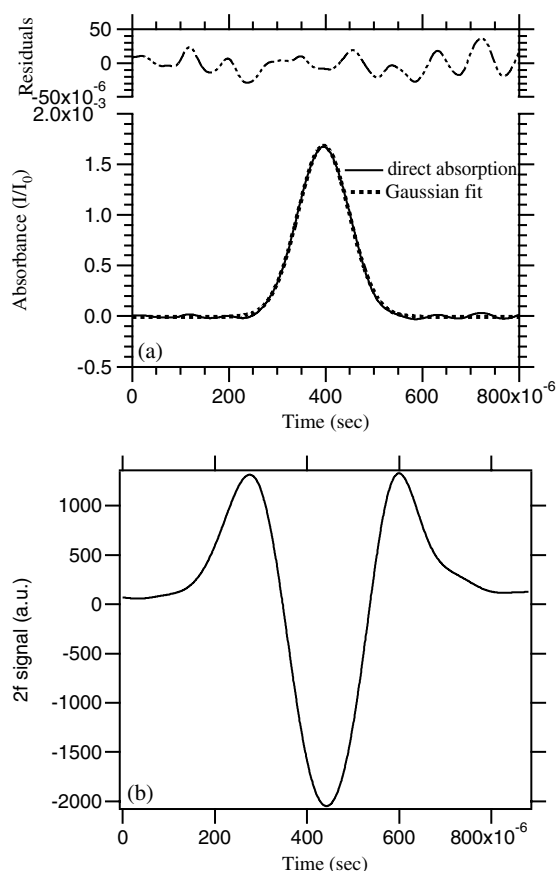


**Figure 3.** Detection of HCl from feedstock flow,  $\text{Cl}_2:\text{HBr} = 10:90$  sccm, without plasma. (a) Direct absorption measurement fit to Doppler lineshape. (b)  $2f$  signal from wavelength modulation detection. Both signals are averaged for 25 scans (50 ms).

to HCl concentration; however, the proportionality constant depends on the modulation index and must be calibrated. The presence of HCl before the plasma is ignited provides a convenient opportunity to use direct absorption for calibration of the  $2f$  wavelength modulation signal. The injection-current modulation of the diode laser also produces a residual amplitude modulation (RAM), and thus the average of two peaks in figure 3(b) is used as a maximum to calculate peak-to-peak value.

The plots in figure 3 are for a typical operating condition with a total feedstock flow rate of 100 sccm, 10:90 ratio of  $\text{Cl}_2:\text{HBr}$ , 10 mTorr chamber pressure, 318 K gas temperature, 50 ms averaging, 500 Hz scan rate, 10.7 MHz modulation frequency, and 2.7 modulation index. For direct absorption measurements, we achieve an  $S = N$  detection limit of  $5 \times 10^{-5}$  peak absorbance with 50 ms averaging (25 scans across the absorption line) and the  $2f$  wavelength modulation detection limit with 50 ms time constant ranged between  $1 \times 10^{-6}$  and  $4 \times 10^{-6}$  for all of the conditions studied here (this reduces to a noise equivalent detection limit between  $2 \times 10^{-7}$  and  $8 \times 10^{-7}/\sqrt{\text{Hz}}$ ).

The feedstock gases were quantitatively converted to HCl via surface chemistry in the plasma chamber and inlet manifold. The gas flows were established for 20 s to allow for flow stabilization and transit time in the manifold. During this

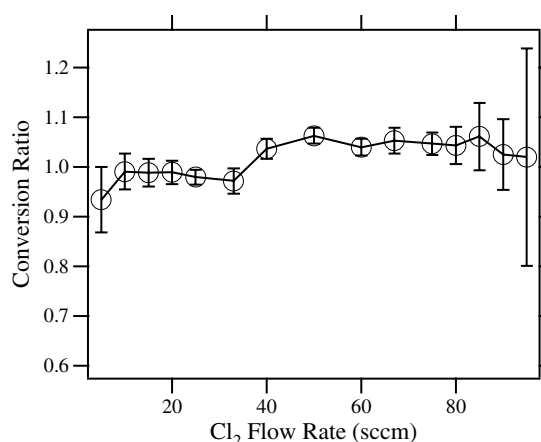


**Figure 4.** Conversion of  $\text{Cl}_2$  and HBr feedstock to HCl without plasma; conversion plotted versus  $\text{Cl}_2$  flow rate for a total flow rate of 100 sccm with the balance HBr for a chamber pressure of 10 mTorr.

time, we find that the gas composition equilibrates, as shown by the measured HCl versus feedstock ratio in figure 4. The data in this figure fall into two regimes. First for flows of  $\text{Cl}_2$  between 0 and 33 sccm, the conversion to HCl is limited by available chlorine, and the data show 100% conversion. For flows of  $\text{Cl}_2$  between 33 and 100 sccm there is not enough hydrogen in the HBr feedstock to convert all the chlorine to HCl, and for this flow range the data consistently show 3–6% more HCl than could be formed from input HBr. We suggest that this is indicative of the amount of water vapour contamination in the etch chamber, gas handling manifold and feedstock gases. This hypothesis is consistent with the performance of the HCl conversion measurements soon after closing the reactor from atmospheric pressure. We would expect water on the gas manifold surfaces to be available for chemical reaction with surface adsorbed  $\text{Cl}_2$ . Thus we conclude there is stoichiometric conversion to HCl from the feedstock of  $\text{Cl}_2/\text{HBr}$  through a surface reaction prior to plasma ignition. Note that the points near 0 and 100%  $\text{Cl}_2$  flow have large uncertainty; at these feedstock compositions the total HCl formed is quite small, and this small signal becomes comparable with the flow meter calibration uncertainties giving rise to large uncertainty in the fractional conversion of the feedstock.

As illustrated in figure 1 above, the transition line strength is a function of rotational temperature; thus, quantitative HCl concentration from absorption measurements requires knowledge of the gas temperature of the neutral species. We have chosen to monitor P(4) for temperature insensitivity in the 350–500 K range. At low pressures in the etch reactor, the absorption lineshape is dominated by Doppler broadening, and from careful lineshape measurements we can measure the translational temperature. We expect the translational and rotational temperatures of HCl to be equal. Several gas flow conditions were explored with a plasma power of 250 W TCP and 350 W TCP. Figure 5(a) shows temperature inferred from the lineshape as a function of  $\text{Cl}_2$  flow rate (100 sccm total feedstock flow with the balance HBr). The translational temperature is found to be relatively constant at  $424 \pm 20$  K under all conditions explored. Note that this is about 100 K higher than the feedstock gas temperature. Since

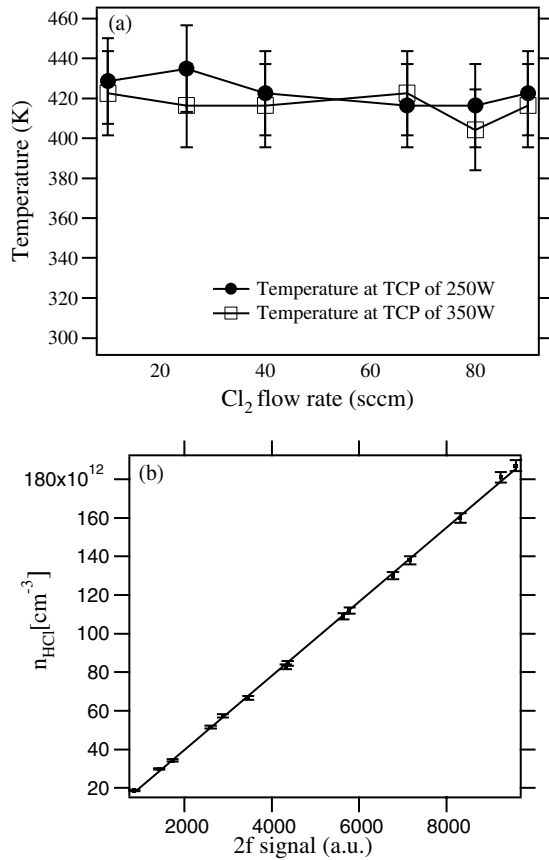


**Figure 5.** (a) Translational temperature deduced from Doppler lineshape of direct absorption during the etching process (b)  $2f$  wavelength modulation signal versus the number density of HCl.

the P(4) transition is temperature insensitive in this temperature region, a single line HCl measurement is accurate within a  $2\sigma$  uncertainty of 5%. This measured translational temperature agrees well with the results of previous literature [21, 25].

After correcting for the gas temperature, the  $2f$  wavelength modulation signal is related to HCl number density using direct-absorption calibration and the measured temperature; and a representative calibration is shown in figure 5(b). As expected for the small absorbance limit, the signal shows good linearity over the entire measurement range between the  $2f$  signal and the direct absorption measurements of HCl number density.

When the plasma is ignited, there is electron impact dissociation of the HCl, and chlorine can be sequestered in SiCl<sub>x</sub>Br<sub>y</sub> etch products. In figure 6, HCl consumption is plotted as a function of Cl<sub>2</sub> and TCP power; HCl consumption defined as  $n_{\text{HCl off}}/n_{\text{HCl on}}$ , with  $n_{\text{HCl off}}$  the number density of HCl in the absence of a plasma and  $n_{\text{HCl on}}$  the number density with the plasma on. The relative HCl consumption is 70–90% at all explored conditions, which agrees well with the measurements of Chou *et al* [22] in HBr plasmas. As the applied rf power increases (TCP power), the dissociation of HCl increases, as expected for higher plasma density.

The TDLAS sensor was used to measure the change in HCl concentration versus the various process parameters. The effect of bias power on the HCl concentration in the plasma is investigated in figure 7. The ion energy is related to bias power,

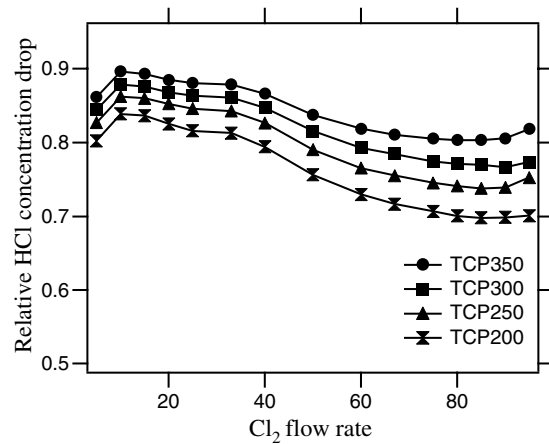


**Figure 6.** Relative concentration drop of HCl when the plasma is ignited at four respective applied power values. Remaining process conditions are 10 mTorr process pressure, lower electrode bias power of 180 W and total flow rate of 100 sccm with the balance HBr.

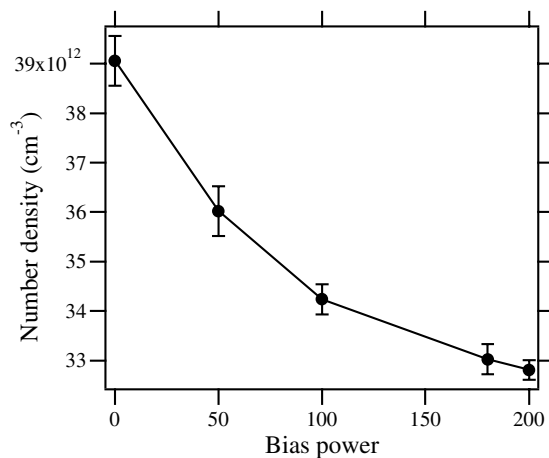


**Figure 7.** Initial HCl concentrations in Cl<sub>2</sub>/HBr plasma versus bias power for 250 W TCP, 10 mTorr, Cl<sub>2</sub>:HBr = 25:75 sccm and total feedstock flow rate of 100 sccm.

and, as the bias power increases, more energetic ions strike the wafer surface. This generally results in a higher etching rate and therefore a larger consumption of chlorine. In addition, increase in bias power should also increase the electron impact dissociation. Thus, the decrease in HCl concentration versus increase in bias power observed in figure 7 is consistent with our interpretation of the HCl concentration as an etch rate monitor.

As shown in figure 8, the HCl number density increases as the total flow rate increases. With the same rf power (TCP) supplied to the plasma at the same pressure, an increase in total flow rate decreases the available energy per mole of feedstock gas resulting in less HCl dissociation. This may account for the observed increase in the HCl number density as total flow rate increases when plasma power is on, although the decreased residence time should tend to decrease the HCl level. The HCl sensor shows that dissociation and dilution dominate with the plasma on, again confirming our interpretation of the plasma chemistry.

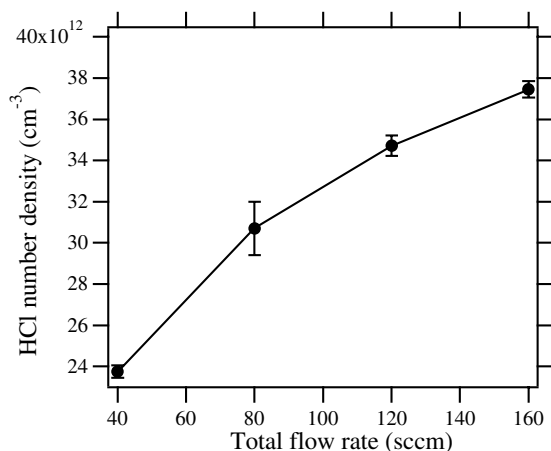


**Figure 8.** Variation of HCl versus total flow rate.

### 5.2. Etch-rate transients observed

The HCl concentration was observed to vary with time after a fluorine-containing etch step was used to remove native oxide; recall that a 20 s  $C_2F_6$  plasma step precedes the  $Cl_2/HBr$  main etch step. We investigated this phenomena measuring HCl with TDLAS and etch rate with real-time spectroscopic ellipsometry (RTSE) [26, 28–31]. During a 2 min main etch process with a  $Cl_2:HBr$  mixture of 10:90 sccm, we observed the time-varying etch rate and HCl chemical concentration variation shown in figure 9. The average etch rate is found to increase as time progresses from about  $1770$  to  $1810 \text{ \AA min}^{-1}$ , while the measured HCl concentration decreases over time from  $15 \times 10^{12}$  to  $9 \times 10^{12} \text{ cm}^{-3}$ . This would correspond to an increase in the HCl consumption from 90 to 94%. As HCl is a reservoir of etching species, such as Cl and  $Cl^+$ , HCl concentration is negatively correlated with the etch rate. This suggests that the HCl concentration may be an indicator or parameter of the chamber state and the etch rate. Note that the chamber walls are also stripped clean of any  $SiO_2$  during the  $C_2F_6$  plasma etch step. Recovery of the etch rate following wall cleaning has been previously reported, and details of the root causes of such transient behaviour are offered in the references for pure Cl plasmas [17–19, 28–31]. However, this is the first such demonstration of related transients seen in the gas composition; here we see the transient in the HCl concentration for  $Cl_2/HBr$  plasmas.

This same transient behaviour, induced by fluorine wall cleaning prior to the main etch  $Cl_2/HBr$  plasma, is also evident in other sensor signals. Exploring these wall disturbance effects further, figure 10 shows four independent sensor signals during a similar 100 s ‘recovery’ etch starting from an F-cleaned chamber condition. The  $Cl_2:HBr$  flow ratio is 80:20 sccm in this case, along with a 5% Ar flow. The remaining plasma conditions are 250 W TCP power, 180 W bias power and 10 mTorr chamber pressure. The top graph of figure 10 plots HCl number density using the TDLAS, which once again starts high and drifts low over the course of the etch. Correspondingly, the real-time etch rate from the RTSE starts low and moves high in the second plot. The third plot tracks plasma density by monitoring the resonance cavity peak position with the broadband rf (BBRF) probe signal. BBRF indicates an initial suppression in density followed by

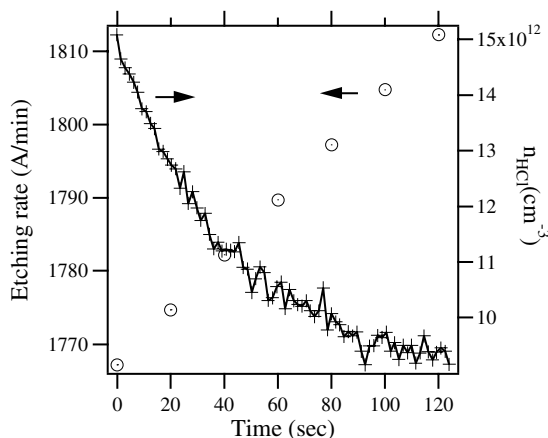


**Figure 9.** Real-time etch rate and HCl  $2f$  signal at  $Cl_2:HBr = 10:90$  sccm, at 10 mT, TCP power of 250 W, and bias power of 180 W. Note, the etch rate varies during the process run.

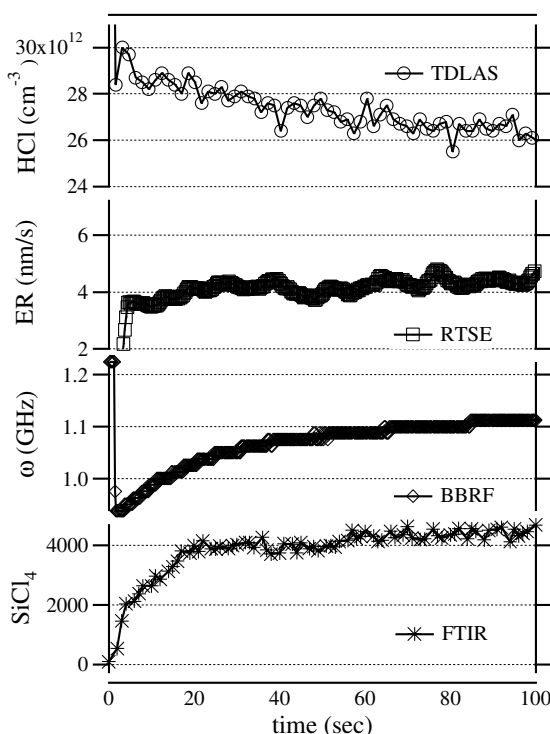


**Figure 10.** All real-time sensors observe time-varying values after the fluorine-containing cleaning step; TDLAS = tunable diode laser absorption spectroscopy for HCl concentration; RTSE = real-time spectroscopic ellipsometry for poly-Si thickness and etch rate; BBRF = broadband rf for electron density; FTIR = Fourier transform infrared spectroscopy for  $SiCl_4$  effluent. Operating condition is  $Cl_2:HBr = 80:20$  sccm, TCP power = 250 W, pressure = 10 mTorr and bias power = 180 W.

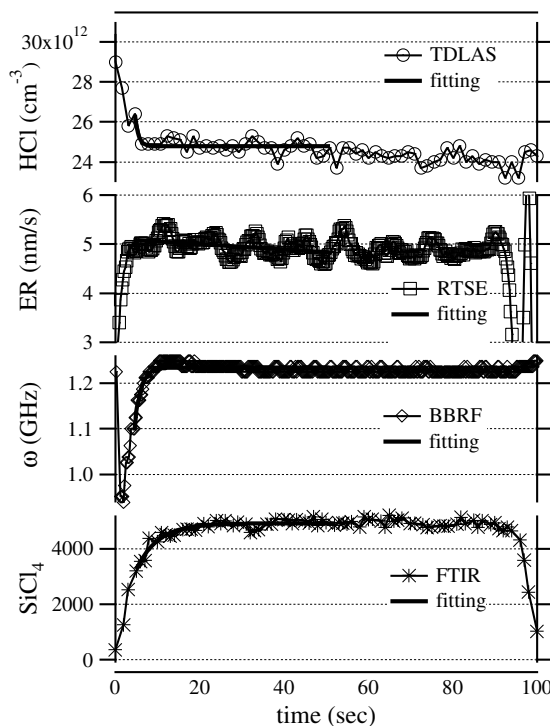
a gradual increase as the etch progresses. Qualitatively, this increase in density is consistent with a concurrent decrease in HCl concentration, as more electrons become liberated to participate in HCl dissociation, thus lowering the concentration over time. Lastly, the final plot measures  $SiCl_4$  effluent from the turbo pump exhaust with an FTIR. Again, qualitatively consistent with the increasing etch rate and plasma density, the  $SiCl_4$  signal is initially suppressed and then rises over the course of the run.

Figure 11 demonstrates a novel feedback control approach to this common process drift problem, maintaining constant plasma density, and first reported for pure  $\text{Cl}_2$  plasmas [28]. Adding feedstock HBr to the  $\text{Cl}_2$  system previously studied, we can use the HCl sensor for direct measurements of HCl concentration during plasma density control. Instead of constant (250 W) TCP input power, we vary the TCP power to maintain a constant plasma density as measured by the BBRF signal. The results in figure 11 clearly demonstrate an improvement in the stability of signals compared to the open-loop experiment in figure 10. Most importantly for the discussion here, in the closed-loop case the HCl number density (upper plot) is noticeably more constant with time than for open-loop experiment. When plasma density is controlled to a constant value throughout the etch cycle, the HCl dissociation fraction, the etch rate, and the  $\text{SiCl}_4$  etch product levels are all significantly more stable with time. The TDLAS sensor illustrates that the plasma composition varies with wall state disturbances and is consistent with the findings of other diagnostics, both during open-loop etch-rate recovery and closed-loop plasma-density-feedback control. The agreement with other sensors and the sensitivity of the measurement demonstrate the potential for optical measurements of HCl concentration for poly-Si etch rate control. Only the BBRF and the TDLAS sensors have sufficient time response and signal-to-noise level to provide the control signal for the closed-loop control needed to maintain constant etch rate.

## 6. Summary

A TDLAS for *in situ* measurements of HCl during poly-Si etching in a commercial plasma etch tool is demonstrated. The wavelength-modulated absorption sensor with 50 ms averaging demonstrated a minimum detectable absorbance of  $4 \times 10^{-6}$  for *in situ* HCl in the  $\text{Cl}_2/\text{HBr}$  etch plasma, corresponding to a minimum detectable HCl concentration of  $\sim 2 \times 10^{11} \text{ cm}^{-3}$ . The translational temperature of HCl was measured at  $424 \pm 20 \text{ K}$  under various  $\text{Cl}_2/\text{HBr}$  flow rates and TCP powers, and did not change significantly over the process regime of interest. When the plasma was ignited, a 70–90% drop in the HCl concentration was observed and this drop increased with higher TCP power due to greater dissociation fractions at higher plasma density. We also observed that increasing bias power decreases the HCl concentration consistent with a correlation of HCl concentration with poly-Si etch rate.

We find that the HCl concentration correlates with measured etch rate. For the first time, we directly observed the time varying etch rate and HCl concentration during the main etch chlorine-based plasma step occurring immediately after the chamber walls were cleaned with a fluorine-based plasma etch step. This implies that for conditions such as those studied here, where HCl concentration in the plasma is correlated with etch rate, an HCl diode laser sensor could be used to monitor and control *in situ* etch rate in such a plasma environment. Finally, the *in situ* diode laser sensor was found to be consistent with independent measurements of real-time etch rate, plasma density and  $\text{SiCl}_4$  variations in both open-loop wall disturbance recovery and closed-loop density controlled etching. The TDLAS sensor signal interpretation is validated by these other sensor measurements over a wide variety of etch



**Figure 11.** Closed-loop control of the plasma power using the BBRF signal after the fluorine-containing cleaning step reduces the time variation of all real-time sensors (identified in the caption for figure 8).

conditions, which illustrates the potential for etch rate control using the TDLAS sensor measurements of HCl concentration.

## Acknowledgments

This research was supported by the Advanced Technology Program administered by the National Institute for Standards and Technology (NIST) via a contract with KLA-Tencor.

## References

- [1] Allen M G 1998 Diode laser absorption sensors for gas-dynamic and combustion flows *Meas. Sci. Technol.* **9** 545–62
- [2] Supplee J M, Whittaker E A and Lenth W 1994 Theoretical description of frequency modulation and wavelength modulation spectroscopy *Appl. Opt.* **33** 6294–302
- [3] Silver J A 1992 Frequency-modulation spectroscopy for trace species detection: theory and comparison among experimental methods *Appl. Opt.* **31** 707–16
- [4] Tuda M, Shintani K and Ootera H 2001 Profile evolution during poly-silicon gate etching with low-pressure high-density  $\text{Cl}_2/\text{HBr}/\text{O}_2$  plasma chemistries *J. Vac. Sci. Technol. A* **19** 711–17
- [5] Collison W-L, Ni T, Chou S-I and Jeffries J B 2001 Silicon etch and process development using diode laser measurements *48th Int. Symp. American Vacuum Society (Boston, MA, Oct. 2001)*
- [6] Lieberman M A and Lichtenberg A J 1994 *Principles of Plasma Discharges and Materials Processing* (New York: Wiley)
- [7] Kovacs G T A 1998 *Micromachines Transducers Sourcebook* (New York: McGraw-Hill)



- [8] Plummer J D, Deal M D and Griffin P B 2000 *Silicon VLSI Technology* (Englewood Cliffs, NJ: Prentice-Hall)
- [9] Semiconductor Industry Association 2001 *International Technology Roadmap for Semiconductors* <http://public.itrs.net/>
- [10] Garvin C, Gilchrist B E, Grimard D S and Grizzle J W 1998 Measurement and error evaluation of electrical parameters at plasma relevant frequencies and impedances *J. Vac. Sci. Technol. A* **16** 595–606
- [11] Garvin C, Grimard D S and Grizzle J W 1998 RF sensing and calibration for real-time control of plasma-based deposition and etching 1998 *Int. Conf. on Characterization and Metrology for ULSI Technology (AIP Conf. Proc. vol 449)* ed D G Seiler *et al* (New York: American Institute of Physics) pp 442–6
- [12] Garvin C, Grimard D S and Grizzle J W 1999 Advances in broad band RF sensing for real-time control of plasma-based semiconductor processing *J. Vac. Sci. Technol. A* **17** 1377–83
- [13] Klimecky P, Grizzle J and Terry F L Jr 2002 Real-time feedback control of plasma density variations in reactive ion etch *AEC/APC 14th Symp. Proc.* <http://www.sematech.org/public/news/conferences/aecapc/orderform.pdf>
- [14] Coburn J W and Chen M 1980 Optical emission spectroscopy of reactive plasmas: a method for correlating emission intensities to reactive particle density *J. Appl. Phys.* **51** 3134–6
- [15] Gottscho R A and Donnelly V M 1984 Optical-emission actinometry and spectral-line shapes in rf glow-discharges *J. Appl. Phys.* **56** 245–50
- [16] Bogart K H A and Donnelly V M 1999 On the constant composition and thickness of the chlorinated silicon surface layer subjected to increasing etching product concentrations during chlorine plasma etching *J. Appl. Phys.* **86** 1822–32
- [17] Ullal S J, Godfrey A R, Edelberg E, Bral L, Vahedi V and Aydil E S 2002 Effect of chamber wall conditions on Cl and Cl<sub>2</sub> concentrations in an inductively coupled plasma reactor *J. Vac. Sci. Technol. A* **20** 43–52
- [18] Donnelly V M 1996 A simple optical emission method for measuring percent dissociations of feed gases in plasmas: application to Cl<sub>2</sub> in a high-density helical resonator plasma *J. Vac. Sci. Technol. A* **14** 1076
- [19] Malyshev M and Donnelly V M 2000 Diagnostics of inductively coupled chlorine plasmas: measurement of Cl<sub>2</sub> and Cl number densities *J. Appl. Phys.* **88** 6207–15
- [20] Sun H C and Whittaker E A 1993 Real-time *in situ* detection of SF<sub>6</sub> in a plasma reactor *Appl. Phys. Lett.* **63** 1035–7
- [21] Sun H C, Patel V, Singh B, Ng C K and Whittaker E A 1994 Sensitive plasma etching endpoint detection using tunable diode laser absorption spectroscopy *Appl. Phys. Lett.* **64** 2779–81
- [22] Chou S, Baer D S, Hanson R K, Collison W Z and Ni T Q 2001 HBr concentration and temperature measurements in a plasma etch reactor using diode laser absorption spectroscopy *J. Vac. Sci. Technol. A* **19** 477–84
- [23] Guelachvili G 1976 Absolute wavenumber measurements of 1–0, 2–0, HF and 2–0, H <sup>35</sup>Cl, H <sup>37</sup>Cl absorption bands *Opt. Commun.* **19** 150–4
- [24] Kaiser E W 1969 Dipole moment and hyperfine parameters of HCl and DCl *J. Chem. Phys.* **53** 1686–703
- [25] Corsi C, Inguscio M, Chudzynski S, Ernst K, D'Amato F and De Rosa M 1999 Detection of HCl on the first and second overtone using semiconductor diode lasers at 1.7 μm and 1.2 μm *Appl. Phys. B* **68** 267–9
- [26] Haverlag M, Stoffels E, Stoffels W W, Kroesen G M W and de Hoog F J 1996 Measurement of the gas temperature in fluorocarbon radio frequency discharges using infrared absorption spectroscopy *J. Vac. Sci. Technol. A* **14** 380–3
- [27] Rothman L S, Rinsland C P, Goldman A, Massie S T, Edwards D P, Flaud J M, Perrin A, Camy-Peyret C, Dana V, Mandin J U, Schroeder J, McCann A, Gamache R R, Wattson R B, Yoshino K, Chance K V, Jucks K W, Brown L R and Nemtchinov V 1996 The Hitran molecular spectroscopic database and Hawks (Hitran atmospheric workstation) *J. Quant. Spectrosc. Radiat. Transfer* **60** 665–710
- [28] Klimecky P I, Grizzle J W and Terry F L Jr 2003 Compensation for transient chamber wall condition using real-time plasma density feedback control in an inductively coupled plasma etcher *J. Vac. Sci. Technol. A* **21** 706–17
- [29] Zau G and Sawin H H 1992 Effects of O<sub>2</sub> feed gas impurity on Cl<sub>2</sub> based plasma etching of poly-silicon *J. Electrochem. Soc.* **139** 250–6
- [30] Huang H T, Kong W and Terry F L Jr 2001 Normal-incidence spectroscopic ellipsometry for critical dimension monitoring *Appl. Phys. Lett.* **78** 3983–5
- [31] Huang H T, Lee J W, Klimecky P I, Khargonekar P P and Terry F L Jr 2001 *In situ* monitoring of deep sub-micron topography evolution and endpoint during reactive ion etching *AEC/APC 13th Symp. Proc.* <http://www.sematech.org/public/news/conferences/aecapc/orderform.pdf>